Defense Technical Information Center Compilation Part Notice

ADP013619

TITLE: Acoustic Propagation Modeling in Shallow Water

DISTRIBUTION: Approved for public release, distribution unlimited

This paper is part of the following report:

TITLE: U.S. Navy Journal of Underwater Acoustics. Volume 51, Number 1, January 2001. Special Feature - The Journal's Fiftieth Anniversary

To order the complete compilation report, use: ADC069959

The component part is provided here to allow users access to individually authored sections of proceedings, annals, symposia, etc. However, the component should be considered within the context of the overall compilation report and not as a stand-alone technical report.

The following component part numbers comprise the compilation report:

ADP013619
ADP205208 thru ADP205213
ADP400167 thru ADP400181

U.S. Navy Journal of Underwater Acoustics Volume 46, No. 4 October 1996

ACOUSTIC PROPAGATION MODELING IN SHALLOW WATER

William A. Kuperman

Scripps Institution of Oceanography
La Jolla, California 92093-0701

(Received April 15, 1996)

This paper provides references for the Navy's existing models for shallow-water propagation. The shallow-water acoustic environment is then briefly described, followed by a description of sound propagation. Four basic models of sound propagation in the ocean most relevant to shallow-water propagation are derived from their common wave equation origin: ray theory, spectral theory, normal mode theory, and the parabolic equation method. Some results from these models are discussed.

INTRODUCTION

The *Oceanographic and Atmospheric Master Library*[1] (OAML) contains a description of Navy models and databases. The Navy's use of shallow-water models can be summarized as follows: Presently, the Navy's standard shallow-water, passive acoustic propagation model, Collosus II, is an empirical fit[1] to observed data. It is used for areas where no significant environmental data are available; otherwise RAYMODE[1] is used for range-independent environments.[2]

For range-dependent environments, the parabolic equation (PE) models[3] are used, including the standard split-step and the more recent finite-element (FEPE) model. ASTRAL[1] is used for higher frequencies, say above 250 Hz. The biggest problem facing shallow-water propagation prediction is the adequacy/resolution of environmental databases. Various compilations of existing models are found in Refs. 1, 4, and 5. The general subject of ocean acoustic modeling and numerical methods is covered in Ref. 3. The purpose of this article is to briefly review the existing shallow-water computer models from the point of view of their physics and their relationship to each other. The frequency regime covered here is up to a few kilohertz. High frequencies do not propagate very long distances, and hence are not dependent on gross shallow-water geophysical properties that comprise the acoustic waveguide. Reference 6 is a compilation of many aspects of high-frequency acoustics.

Although shallow-water acoustics has received great attention recently, there already is a rich baseline knowledge of acoustic propagation. Great progress has been made in understanding this subject since the Bradley-Urick[7] compilation of transmission loss for various shallow-water scenarios appeared. The plots in this latter reference showed a 40 dB spread at 10 km and a 50 dB spread at 100 km. In this paper, we review the progress in modeling sound propagation in shallow water and the subsequent understanding that modeling and data analysis has provided. The bottom line is that the environmental inputs to acoustic models remain the crucial factor for quantitatively predicting propagation conditions.

We start this paper with a qualitative description of sound propagation in shallow water. Next we describe the generic propagation models in enough detail to give the reader a sense of both their common underlying physics and their different theoretical and algorithmic approaches. We conclude the paper with illustrative results from the various models.

UNCLASSIFIED

DESCRIPTIVE SHALLOW-WATER ACOUSTICS

In this section we describe the basic features of shallow-water environments and how these features control sound propagation.[3,8,9] See the Appendix for discussion of units.

Environment

By shallow water, this author means continental shelf and slope such that sound propagation is best described as a waveguide phenomenon. The waveguide is defined by the upper air-sea boundary and the ocean bottom interface, which in a more general sense may be a composite of stratified and/or nonstratified layers. The latter is often called a range-dependent environment that also includes the case of the sound speed varying as a function of horizontal position, not just depth. The acoustic modeling significance of a range-dependent environment is that the wave equation describing acoustic propagation is not a "separable" partial differential equation, and therefore usually requires more computationally intensive methods than separable equations.

The two most common classes of sound speed profiles in shallow water are schematically represented in Fig. 1. Typically, much of what is classified as shallow water is not deep enough for the depth-pressure term in the temperature-salinity-pressure dependence of sound speed to be significant. Thus the winter profile tends to isovelocity simply because of mixing, whereas the summer profile has a higher sound speed near the surface due to heating. The sound speed profile may vary spatially and temporally. Often, the temporal variations are caused by internal wave fields that tend to be more ordered in shallow water than in deep water. Sometimes confined internal wave packets, referred to as solitons, produce localized, travelling ocean disturbances.

The ocean bottom has a great impact on sound propagation due to its material properties. Table 1 summarizes some of the acoustic properties of the ocean bottom.[3] The effects of these bottom properties are briefly described in the next subsection.

Acoustics

Much of the qualitative behavior of sound in shallow water can be described by a combination of a simple application of Snell's law and some understanding of the reflection properties of the ocean bottom. Basically, Snell's law states that sound bends toward regions of low sound speed. Hence, as described above, summer sound speed

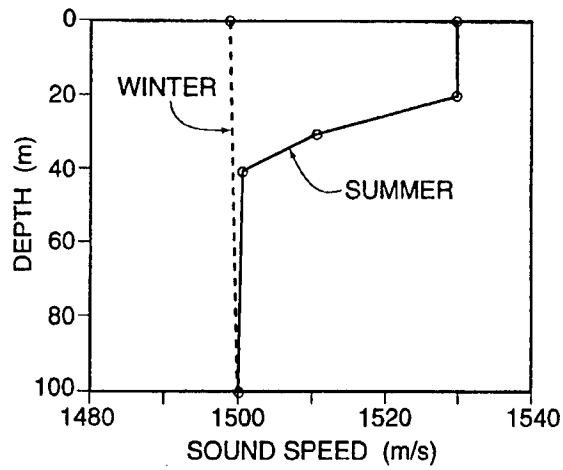

Fig. 1 — Typical summer and winter sound speed profiles

profiles produce rays that bend more toward the bottom than winter profiles in which the rays tend to be straight. This implies two effects with respect to the ocean bottom:

- for a given range, there are more bounces off the ocean bottom in summer than in the winter; and
- the ray angles intercepting the bottom are steeper in the summer than in the winter.

A qualitative understanding of the reflection properties of the ocean bottom should therefore be very revealing of sound propagation in summer vs winter. Basically, near-grazing incidence is much less lossy than larger, more vertical angles of incidence. Because summer condition propagation paths have more bounces, each of which are at steeper angles than winter paths, we can expect summer shallow-water propagation to be much worse than in winter conditions, which indeed they are. This result is often tempered by rough winter sea surface conditions that generate large scattering losses at the higher frequencies.

Bottom Loss

Modeling the shallow-water environment as a waveguide yields a qualitative description of sound propagation that is very helpful in understanding more sophisticated model outputs. However, to understand the effects of the ocean bottom, let us first review the reflection properties of an interface separating two media.

Ocean bottom sediments are often modeled as fluids since the rigidity (and hence the shear speed) of the sediment is usually considerably less than that of a solid, such

UNCLASSIFIED

UNCLASSIFIED

UNCLASSIFIED

Table 1 — Geoacoustic Properties of Shallow Water and Continental Slope Ocean Bottoms
(θz is the depth below the water-bottom interface)

Bottom Type	p (%)	$\rho b/\rho w$	c_p/c_w	c_p (m/s)	c_s (m/s)	a_b (dB/λ_p)	a_s (dB/λ_s)
Clay	70	1.5	1.00	1500	<100	0.2	1.0
Silt	55	1.7	1.05	1575	$c_s^{(1)}$	1.0	1.5
Sand	45	1.9	1.1	1650	$c_s^{(2)}$	0.8	2.5
Gravel	35	2.0	1.2	1800	$c_s^{(3)}$	0.6	1.5
Moraine	25	2.1	1.3	1950	600	0.4	1.0
Chalk	—	2.2	1.6	2400	1000	0.2	0.5
Limestone	—	2.4	2.0	3000	1500	0.1	0.2
Basalt	—	2.7	3.5	5250	2500	0.1	0.2

$c_s^{(1)} = 80\ \bar{z}^{0.3}$ $\quad c_s^{(3)} = 180\ \bar{z}^{0.3}$

$c_s^{(2)} = 100\ \bar{z}^{0.3}$ $\quad c_w = 1500$ m/s, $\rho_w = 1000$ kg/m^3

as rock. In the latter case, which applies to the "ocean basement" or the case where there is no sediment overlying the basement, the medium must be modeled as an elastic solid. This means that it supports both compressional and shear waves.

Reflectivity, the amplitude ratio of reflected and incident plane waves at an interface separating two media, is an important measure of the effect of the bottom on sound propagation. For an interface between two fluid semi-infinite halfspaces with density ρ_i and sound speed c_i, i = 1,2, and a unit amplitude incident wave of the form exp $[i(k_\perp r + k_{1z} z) - i\omega t]$ [Fig. 2(a)], the reflectivity is given by

$$R(\theta) = \frac{\rho_2 k_{1z} - \rho_1 k_{2z}}{\rho_2 k_{1z} + \rho_1 k_{2z}}, \qquad (1)$$

with

$$k_{iz} = (\omega/c_i) \sin \theta_i \equiv k_i \sin \theta_i;\ i = 1,2. \qquad (2)$$

The incident and transmitted grazing angles are related by Snell's law,

$$k_\perp = k_1 \cos \theta_1 = k_2 \cos \theta_2, \qquad (3)$$

where the incident grazing angle θ_1 is also equal to the angle of the reflected plane wave. $R(\theta)$ is also referred to as the Rayleigh reflection coefficient, and has unit magnitude (total internal reflection) when the numerator and denominator of Eq. (1) are complex conjugates. This occurs when k_{2z} is purely imaginary. Using Snell's law, Eq. (3), for determining θ_2 in terms of the incident grazing angle, we obtain the critical grazing angle below which there is perfect reflection,

$$\cos \theta_c = c_1/c_2, \qquad (4)$$

so that a critical angle can exist only when the speed in the second medium is higher than that of the first. Below the critical angle, the reflected wave undergoes a change of phase ϵ, given by the argument of the complex reflection coefficient; in this region [and using Eq. (2)], the reflection coefficient can be written as a complex number with unit magnitude

UNCLASSIFIED

UNCLASSIFIED

UNCLASSIFIED

$$R(\theta) = \frac{\dfrac{\rho_2}{\rho_1} + i\dfrac{\sqrt{\cos^2\theta_1 - (c_1^2/c_2^2)}}{\sqrt{1 - \cos^2\theta_1}}}{\dfrac{\rho_2}{\rho_1} - i\dfrac{\sqrt{\cos^2\theta_1 - (c_1^2/c_2^2)}}{\sqrt{1 - \cos^2\theta_1}}} \equiv e^{i\epsilon}, \quad (5)$$

where

$$\epsilon = 2\tan^{-1}\frac{\rho_1\sqrt{\cos^2\theta_1 - (c_1^2/c_2^2)}}{\rho_2\sqrt{1 - \cos^2\theta_1}}. \quad (6)$$

Note that $\rho_2 = 0$ is the pressure release case, which is a good approximation to that water/air interface; for this case there is a 180-deg phase change. For the two-fluid interface under consideration, the phase change goes from 180 deg at horizontal grazing incidence to no phase change at the critical angle. On the other hand, when the density and speed of the second medium is very large, corresponding to the rigid interface condition, there is no phase change. Since it turns out that most shallow-water propagation corresponds to paths with very low grazing angles, the pressure release condition is actually a better approximation of a two-fluid interface than the rigid boundary condition.

Using Eq. (2), Eq. (1) can also be rewritten as

$$R(\theta) = \frac{\rho_2\, c_2/\sin\theta_2 - \rho_1\, c_1/\sin\theta_1}{\rho_2\, c_2/\sin\theta_2 + \rho_1\, c_1/\sin\theta_1} \equiv \frac{Z_2 - Z_1}{Z_2 + Z_1}, \quad (7)$$

where the right-hand side is in the form of impedances $Z_i(\theta_i) = \rho_i c_i/\sin\theta_i$, which are the ratios of the pressure to the vertical particle velocity at the interface in the ith medium. Written in this form, more complicated reflection coefficients become intuitively plausible. Consider the case in Fig. 2(a) in which the second medium is elastic and thus supports shear as well as compressional waves with sounds speeds c_{2s} and c_{2p}, respectively. The Rayleigh reflection coefficient is then given by

$$R(\theta) = \frac{Z_{2tot} - Z_1}{Z_{2tot} + Z_1}, \quad (8)$$

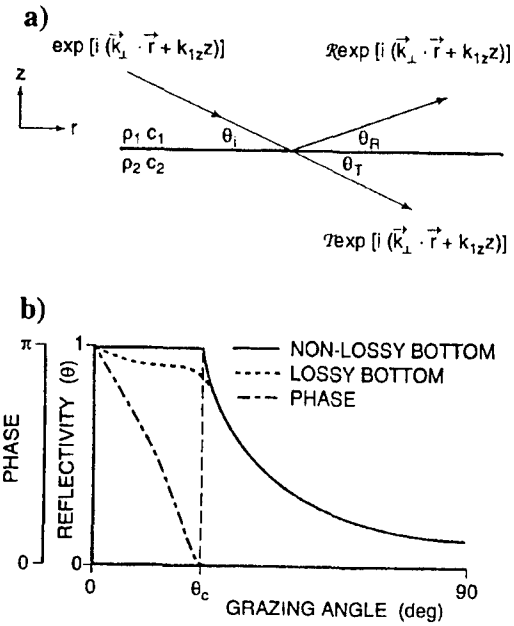

Fig. 2 — The reflection and transmission process

with the total impedance of the second medium being

$$Z_{2tot} \equiv Z_{2s}\sin^2 2\theta_{2s} + Z_{2p}\cos^2 2\theta_{2s}. \quad (9)$$

Snell's law for this case is

$$k_1\cos\theta_1 = k_{2s}\cos\theta_{2s} = k_{2p}\cos\theta_{2p}. \quad (10)$$

Shear speeds of less than a few hundred m/s have very little effect on sound propagation. However, sediments with shear speeds greater than a few hundred m/s but still much lower than the speed of sound in water (say, up to 1000 m/s) appear to be highly absorbing because the propagation of shear waves is another degree of freedom for sound to be transmitted away from the water column. For even greater shear speeds but still less than the speed of sound in water, the bottom appears almost transparent and waveguide propagation is severely attenuated. For the case of the shear speed exceeding the sound speed in water, the shear speed is the dominant bottom sound speed parameter because its value is closest to the water sound speed (the bottom compressional speed must be larger than the shear speed). For this case, a reasonable approximation (which also

UNCLASSIFIED

UNCLASSIFIED

neglects the existence of interface waves) to the magnitude of the bottom reflectivity is to treat the ocean bottom as an effective fluid whose compressional speed is the shear speed of the elastic bottom. Thus, the ratio of the shear speed to the water sound speed will determine the critical angle.

In lossy media, attenuation can be included in the reflectivity formula by taking the sound speed as complex so that the wavenumbers are subsequently also complex, $k_i \rightarrow k_i + \alpha_i$. Figure 2(b) depicts a simple bottom loss curve derived from the Rayleigh reflection coefficient formula. Both the densities and sound speed of the second medium are larger than those in the first medium, with unit reflectivity indicating perfect reflection. The phase change upon reflection is also shown. For loss in dB, 0 dB is perfect reflecting, 6 dB loss is an amplitude factor of one-half, 12 dB loss is one-fourth, etc. For a lossless bottom, severe loss occurs above the critical angle in the water column due to transmission into the bottom. For the lossy (more realistic) bottoms, only partial reflection occurs at all angles. With paths involving many bottom bounces (shallow-water propagation), bottom losses as small as a few-tenths of a dB per bounce accumulate and become significant because the propagation path may involve many tens of bounces. A description of a reflectivity database is given in Section 2.2.8 of Ref. 1.

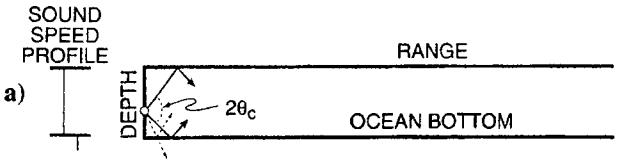

(a) Long-distance propagation occurs within a cone of $2\theta_c$

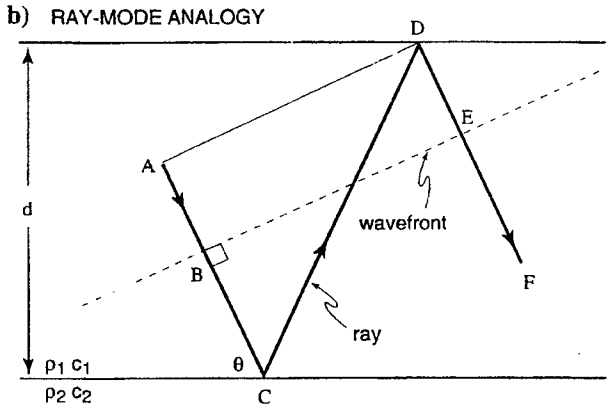

(b) Geometry for the constructive interference of wavefronts to form a mode

Fig. 3 — Ocean waveguide propagation

Qualitative Description of Waveguide Propagation

For simplicity, we consider an isovelocity waveguide bounded above by the air/water interface and below by a two-fluid interface. Hence, we will have perfect reflection, with a 180-deg phase change at the surface. For paths more horizontal than the bottom critical angle, there will also be perfect reflection with an angle-dependent phase change given by Eq. (6). Therefore, as schematically indicated in Fig. 3(a), ray paths within a cone of 2 θ_c will propagated unattenuated down the waveguide. Because the up and down going rays have equal amplitudes, preferred angles will exist such that perfect constructive interference can occur. These particular angles can be associated with the normal modes of the waveguide as formally derived from the wave equation in the next section. However, it is instructive to understand the geometric origin of the waveguide modal structure.

Figure 3(b) is a schematic of a ray reflected from the bottom and then the surface of a "Pekeris" waveguide (an environment with constant sound speeds and densities in the water column and fluid bottom, respectively). Consider a ray along the path ACDF and its wavefront, which is perpendicular to the ray. The two down-going rays, AC and DF, which are of the form

$$\phi_{down,up} \approx \exp\left[i(k_\perp r \pm k_{1z} z) - i\omega t\right] \qquad (11)$$

will constructively interfere if points B and E have a phase difference of an integral number of 360 deg (and similarly for up-going rays). The acoustic phase change along BCDE is given by the product of the wavenumber and the distance along the ray plus the change of phase at C and a 180-deg phase change at D, the pressure release surface. Noting that $\overline{AB} = \overline{DE}$, the condition for constructive interference is

UNCLASSIFIED

$$k\left[\frac{d}{\sin\theta_n} - \frac{d}{\sin\theta_n}\cos(\pi - 2\theta_n)\right] \qquad (12)$$
$$+ \epsilon + \pi = 2(n-1)\pi;\ n = 1,2,\ldots,$$

which, after using Eq. (6), reduces to

$$\tan\left(d\sqrt{k_1^2 - k_n^2}\right) = -\frac{\rho_2}{\rho_1}\frac{\sqrt{k_n^2 - k_1^2}}{\sqrt{k_2^2 - k_n^2}}, \qquad (13)$$

where k_n is the horizontal wavenumber, $k_\perp$, corresponding to the discrete angle θ_n and we have converted from angles to wavenumbers by using the relations $c_1/c_2 = k_2/k_1$ and $k_{1z} = \sin\theta_n = \sqrt{k_1^2 - k_n^2}$.

Equation (13) is a transcendental equation in k_n with real roots in the range

$$k_2 < k_n < k_1; \qquad (14)$$

k_n can be thought of as a wavenumber of a horizontal wave traveling down the waveguide with a phase velocity of $c_n = \omega/k_n$. Figure 3(b) shows that the more vertical the ray, the more horizontal the wavefront. Hence, a vertical ray corresponds to a horizontal wavefront, and the horizontal phase velocity along such a wavefront must be infinite since the wavefront has constant phase. However, Ineq. (14) limits the phase velocity to a maximum of c_2, that is, rays more vertical than the critical angle do not propagate (more than a few bounces) down the waveguide. (For the simple limiting case of a waveguide bounded above and below by pressure release surfaces, the rays do approach the vertical so that the horizontal phase velocity c_n goes to infinity with increasing mode number n.) On the other hand, a horizontal ray has a vertical wavefront, and so the phase is constant in the vertical. In this case, the horizontal phase velocity is limited to the medium speed. The vertical amplitude of the wave can be obtained by looking at the z part of the fields described by Eq. (11). The field for a particular n will be a superposition of the up and downgoing fields of Eq. (11). However, we need a negative sign between the two amplitudes so that the field vanishes at the surface. The result is that the superposition of discrete up and downgoing waves results in a vertical amplitude distribution in the waveguide of the form,

$$\phi_n \approx e^{i(k_n r - \omega t)} u_n(z); \quad u_n(z) = \sin\left(\sqrt{k_1^2 - k_n^2}\, z\right). \qquad (15)$$

The u_n's are called the normal modes of the waveguide, and they each propagate with phase velocity c_n. The total field in the waveguide is the sum of all the normal mode terms in Eq. (15). The vertical distribution can be thought of as a superposition of up and downgoing plane waves at discrete propagation angles within the cone $\pm\theta_c$. This discussion is qualitatively correct in general, but is quantitatively limited to an isovelocity water column overlying a fluid bottom with a constant soundspeed, i.e., a Pekeris waveguide. In the next section we show that Eq. (13) is the eigenvalue equation that comes from normal mode theory. If the bottom medium is attenuating, then the wavenumber in the bottom will be complex. In this case, the individual eigenvalues k_n become complex, and there is an additional factor of $\exp(-\alpha_n r)$ multiplying Eq. (15). Physically, the normal mode attenuation coefficients α_n increase with n since the higher order modes are more vertical and therefore correspond to rays that have greater loss per bounce and more bounces per distance down the waveguide.

A simple limiting case is when we approximate the bottom as pressure release. The density of the second medium vanishes so that the right-hand side of Eq. (13) is zero. This reduces to $d\sqrt{k_1^2 - k_n^2} = n\pi$ so that the normal mode functions of this waveguide, the π phase-shifted sum of the up and down going waves of Eq. (11), is of the form $\sin(n\pi z/d)$, which are a set of orthogonal functions that vanish at both surfaces.

SOUND PROPAGATION MODELS

Sound propagation in the ocean is mathematically described by the wave equation, whose parameters and boundary conditions are descriptive of the ocean environment.[3] There are essentially four types of models (computer solutions to the wave equation) to describe sound propagation in the sea: ray theory, the spectral or fast field program (FFP), normal mode (NM), and parabolic equation (PE). All of these models allow for the fact that the ocean environment varies with depth. A model that also takes into account horizontal variations in the environment (i.e., sloping bottom or spatially variable oceanography) is termed range-dependent. For high frequencies (a few kilohertz or above), ray theory is the most practical. The other three model types are more applicable and usable at lower frequencies (below a kilohertz). The hierarchy of underwater acoustics models is shown in schematic form in Fig. 4.

UNCLASSIFIED

UNCLASSIFIED

UNCLASSIFIED

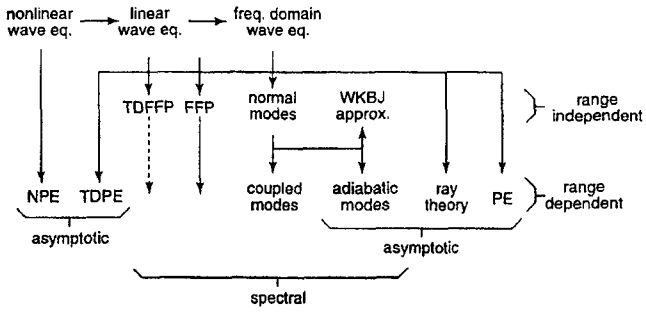

Fig. 4 — Hierarchy of underwater acoustics models (note: "TD" refers to time domain)

The Wave Equation and Boundary Conditions

The wave equation is typically written and solved in terms of pressure, displacement, or velocity potentials. For a velocity potential φ, the wave equation in cylindrical coordinates with the range coordinates, denoted by $\mathbf{r} = (x,y)$, and the depth coordinate denoted by z (taken positive downward) for a source free region is

$$\nabla^2\varphi(\mathbf{r},z,t) - \frac{1}{c^2}\frac{\partial^2\varphi(\mathbf{r},z,t)}{\partial t^2} = 0, \qquad (16)$$

where c is the sound speed in the wave propagating medium. With respect to the velocity potential, the velocity $\mathbf{v}$ and pressure p are given by

$$\mathbf{v} = \nabla\varphi, \quad p = -\rho\frac{\partial\varphi}{\partial t}, \qquad (17)$$

where ρ is the density of the medium. The wave equation is most often solved in the frequency domain, that is, a frequency dependence of $\exp(-i\omega t)$ is assumed to obtain the Helmholtz equation ($K \equiv \omega/c$),

$$\nabla^2\varphi(\mathbf{r},z) + K^2\varphi(\mathbf{r},z) = 0. \qquad (18)$$

In underwater acoustics, both fluid and elastic (shear supporting) media are of interest. In elastic media, the field can be expressed in terms of three scalar displacement potentials, $\phi(\mathbf{r}, z)$, $\psi(\mathbf{r}, z)$, and $\Lambda(\mathbf{r}, z)$, corresponding to compressional (P), vertically polarized (SV), and horizontally polarized shear waves (SH), respectively. In the limiting case of a fluid medium, where shear waves do not exist, $\Phi(\mathbf{r}, z)$ represents the compressional potential $\phi(\mathbf{r}, z)$. Most underwater acoustic applications involve only compressional sources, which only excite the P and SV potentials, eliminating the SH potential $\Lambda(\mathbf{r}, z)$. The displacement potentials satisfy the Helmholtz equation with the appropriate compressional or shear sound speeds c_p or c_s, respectively,

$$c_p = \left[\frac{\lambda + 2\mu}{\rho}\right]^{1/2}, \quad c_s = \left[\frac{\mu}{\rho}\right]^{1/2}, \qquad (19)$$

where λ and μ are the Lamé constants.

The most common plane interface boundary conditions encountered in underwater acoustics are described below: For the ocean surface, there is the pressure release condition where the pressure (normal stress) vanishes; for the appropriate solution of the Helmholtz equation, this conditions is

$$p = 0, \varphi = 0 \text{ or } \phi = 0. \qquad (20)$$

The interface between the water column (layer 1) and an ocean bottom sediment (layer 2) is often characterized as a fluid-fluid interface. The continuity of pressure and vertical particle velocity at the interface yields the following boundary conditions in terms of pressure:

$$p_1 = p_2, \quad \frac{1}{\rho_1}\frac{\partial p_1}{\partial z} = \frac{1}{\rho_2}\frac{\partial p_2}{\partial z}, \qquad (21)$$

or velocity potential:

$$\rho_1\varphi_1 = \rho_2\varphi_2, \quad \frac{\partial\varphi_1}{\partial z} = \frac{\partial\varphi_2}{\partial z}. \qquad (22)$$

These boundary conditions applied to the plane wave fields in Fig. 2(a) yield the Rayleigh reflection coefficient given by Eq. (1).

For an interface separating two solid layers, the boundary conditions are continuity of vertical displacement $w(\mathbf{r}, z_i)$, tangential displacements $\mathbf{u}(\mathbf{r}, z_i) = (u_x, u_y)$, normal stress $n = \sigma_{zz}$, and tangential stresses $\mathbf{t} = (\sigma_{xz}, \sigma_{yz})$. In cylindrical coordinates with azimuthal symmetry, the radial

UNCLASSIFIED

UNCLASSIFIED

UNCLASSIFIED

and vertical components of displacements (in homogeneous media) u and w, respectively, are

$$u(r,z) = \frac{\partial \phi}{\partial r} + \frac{\partial^2 \psi}{\partial z^2}, \tag{23}$$

$$w(r,z) = \frac{\partial \phi}{\partial z} - \frac{1}{r}\frac{\partial}{\partial r} r \frac{\partial \psi}{\partial r}, \tag{24}$$

and the normal and tangential stresses are

$$\sigma_{zz}(r,z) = (\lambda + 2\mu)\frac{\partial w}{\partial z} + \lambda \frac{\partial u}{\partial r}, \tag{25}$$

$$\sigma_{r,z} = \mu \left[\frac{\partial u}{\partial z} + \frac{\partial w}{\partial r}\right]. \tag{26}$$

Continuity of these quantities at the interface between two solids are the boundary conditions. For a fluid-solid interface, the rigidity μ vanishes in the fluid layer, and the tangential stress in the solid layer vanishes at the boundary. If at least one of the media is elastic, these boundary conditions permit the existence of interface or surface waves, such as Rayleigh waves, at the interface between a solid and vacuum, Scholte waves at a fluid-solid interface, and Stoneley waves at a solid-solid interface. These waves are excited when the source is acoustically close, in terms of wavelengths, to the interface.

The Helmholtz equation for an acoustic field from a point source with angular frequency ω is

$$\nabla^2 G(\mathbf{r},z) + K^2(\mathbf{r},z) = -\delta^2(\mathbf{r} - \mathbf{r}_s)\,\delta(z - z_s);$$
$$K^2(\mathbf{r},z) = \frac{\omega^2}{c^2(\mathbf{r},z)}, \tag{27}$$

where the subscript "s" denotes the source coordinates. The range-dependent environment manifests itself as the coefficient $K^2(\mathbf{r},z)$ of the partial differential equation for the appropriate sound speed profile. The range-dependent bottom type and topography appear as boundary conditions on scalars and tangential and normal quantities, as discussed above.

Ray Theory

Ray theory[10] is a geometrical, high-frequency approximate solution to Eq. (27) of the form

$$G(\mathbf{R}) = A(\mathbf{R}) \exp[iS(\mathbf{R})], \tag{28}$$

where the exponential term allows for rapid variations as a function of range, and $A(\mathbf{R})$ is a more slowly varying "envelope" that incorporates both geometrical spreading and loss mechanisms. The geometrical approximation is that the amplitude varies slowly with range (i.e., $(1/A)\nabla^2 A << K^2$), so that Eq. (27) yields the eikonal equation

$$(\nabla S)^2 = K^2. \tag{29}$$

The ray trajectories are perpendicular to surfaces of constant phase (wavefronts) S, and may be expressed mathematically as

$$\frac{d}{dl}\left[K \frac{d\mathbf{R}}{dl}\right] = \nabla K, \tag{30}$$

where l is the arc length along the direction of the ray and $\mathbf{R}$ is the displacement vector. The direction of average flux (energy) follows that of the trajectories, and the amplitude of the field at any point can be obtained from the density of rays. See chapter 3 of Ref. 3 for more details.

The ray theory method is computationally rapid and extends to range-dependent problems. Furthermore, the rays give a physical picture of the acoustic paths. It is helpful in describing how noise redistributes itself when propagating long distances over paths that include shallow and deep environments and/or mid-latitude to polar regions. The disadvantage of conventional ray theory is that it does not include diffraction and such effects that describe the low-frequency dependence ("degree of trapping") of ducted propagation. In shallow water, many rays with many bottom bounces are required. Hence, small errors from the high-frequency approximation will accumulate rapidly with range.

Full Field Solution or "Fast Field Program (FFP)"

The wave equation can be solved efficiently with spectral methods[3] when the ocean environment does not

UNCLASSIFIED

UNCLASSIFIED

vary with range. The term "Fast Field Program" is used because the spectral methods became practical with the advent of the fast Fourier transform (FFT). Assuming a solution of Eq. (27) of the form

$$G(\mathbf{r},z) = \frac{1}{2\pi}\int_{-\infty}^{\infty} d^2\mathbf{k}\, g(\mathbf{k},z,z_s) \exp[i\mathbf{k}\cdot(\mathbf{r}-\mathbf{r}_s)] \quad (31)$$

leads to an equation for the depth-dependent Green's function $g(\mathbf{k}, z, z_s)$,

$$\frac{d^2g}{dz^2} + (K^2(z) - k^2)\, g = -\frac{1}{2\pi}\,\delta(z - z_s). \quad (32)$$

Furthermore, we assume azimuthal symmetry $kr > 2\pi$ and $\mathbf{r}_s = 0$ so that Eq. (31) reduces to (after integrating over the azimuthal angle and converting the Bessel function to Hankel functions and using the asymptotic form of the Hankel function ($H_0^1(kr) \to \sqrt{(2/\pi kr)}\exp[ikr - \pi/4)]$)

$$G(r,z) = \frac{\exp(-i\pi/4)}{(2\pi r)^{1/2}}\int_0^{\infty} dk\,(k)^{1/2} g(k,z,z_s)\exp(ikr). \quad (33)$$

We now convert the above integral to an FFT form by setting $k_m = k_0 + m\Delta k$; $r_n = r_0\ n\Delta r$ where $n, m = 0, 1, \ldots N\text{-}1$ with the additional condition $\Delta r \Delta k = 2\pi/N$ where N is an integral power of two:

$$G(r_n,z) = \frac{\Delta k \exp[i(k_0 r_n - \pi/4)}{(2\pi r)^{1/2}} \times \sum_{m=0}^{N-1} X_m \exp(2\pi i m n/N), \quad (34)$$

$$X_m = (k_m)^{1/2} g(k_m,z,z_s)\ \exp\ (i m r_0 \Delta k).$$

Although the method is labeled "fast field," it is fairly slow because of the time required to calculate the Green's functions [solve Eq. (32)] many times. However, it has advantages when one wishes to calculate the "near field" region or to include shear wave effects in elastic media.[11,12] It is also often used as a benchmark for other less exact techniques. We show below the relationship between the structure of $g(k,z,z_s)$ and the normal modes of the waveguide. This spectral solution technique has recently been extended to include range-dependent environments.[13]

For completeness, we mention an alternative method[14,15] to evaluate Eq. (31) using a raylike representation solution [Eq. (32)]. Up and downgoing solutions that satisfy the upper and lower boundary conditions are constructed by using the appropriate boundary reflection coefficients. The result is an infinite sum of multiple bouncing rays. Although often such solutions are awkward for shallow-water problems (too many bounces combined with approximation errors), circumstances that involve reverberation formulated in terms of scattering at specific bounce locations can be handled with such a technique.

Normal Mode Model (NM)

Rather than evaluate Eq. (32) for each g for the complete set of ks [typically solving Eq. (32) 1024 to 8196 times], one can utilize a normal mode expansion of the form

$$g(\mathbf{k},z) = \sum a_n(\mathbf{k}) u_n(z), \quad (35)$$

where the quantities u_n are eigenfucntions of the following eigenvalue problem:

$$\frac{d^2u_n}{dz^2} + [K^2(z) - k_n^2]\, u_n(z) = 0; \qquad \int_0^{\infty} \frac{u_m(z)u_n(z)}{\rho(z)}\, dz = \delta_{nm}, \quad (36)$$

where $\delta_{nm} = 1$ for $n = m$ and is zero for $n \neq m$. The eigenfunctions u_n are zero at $z = 0$, satisfy the local boundary conditions descriptive of the ocean bottom properties, and satisfy a radiation condition for $z \to \infty$. They form an orthonormal set in a Hilbert space with weighting function $\rho(z)$, the local density. Thus, for example, in a Pekeris waveguide, K is $\omega/c_{1,2}$, where $c_{1,2}$ is the speed of sound in the water and bottom, respectively, and Eq. (36) is solved with the boundary conditions given by Eqs. (20) and (21). For the eigenvalues and eigenfunction, the solution is Eqs. (13) and (15) [with an additional normalization factor for Eq. (15) resulting from the orthonormality condition of Eq. (36)].

The range of discrete eigenvalues is given by the condition

$$\min[K(z)] < k_n < \max[K(z)]. \quad (37)$$

UNCLASSIFIED

This is the nonisovelocity generalization of Ineq. (14). These discrete eigenvalues correspond to discrete angles within the critical angle cone in Fig. 3(a) such that specific waves constructively interfere. The eigenvalues k_n typically have a small imaginary part α_n, which serves as a modal attenuation coefficient representative of all the losses in the ocean environment (see Ref. 3 for the formulation of normal mode attenuation coefficients, and other references). Solving Eq. (32) by using the normal mode expansion given by Eqs. (35) and (36) permits an analytic integration of Eq. (31) yielding (for the source at the origin)

$$G(r,z) = \frac{i}{4}\rho(z_s)\sum_n u_n(z_s)u_n(z)H_0^1(k_n r). \quad (38)$$

The asymptotic form of the Hankel function [given above Eq. (33)] can be used in the above equation to obtain the well-known normal mode representation of a cylindrical (axis is depth) waveguide:

$$G(r,z) = \frac{i\rho(z_s)}{(8\pi r)^{1/2}}\exp(-i\pi/4) \times \sum_n \frac{u_n(z_s)u_n(z)}{k_n^{1/2}}\exp(ik_n r - \alpha_n r), \quad (39)$$

with the modal attenuation coefficient given by

$$\alpha_n = \frac{\alpha}{k_n}\int_d^\infty \frac{K(z)|u_n(z)|^2}{\rho(z)}. \quad (40)$$

Equation (39) is a far field solution of the wave equation and neglects the continuous spectrum ($k_n < \min[K(z)]$ of Ineq. (37)].

To illustrate the various portions of the acoustic field, we note that k_n is a horizontal wave number so that a "ray angle" associated with a mode with respect to the horizontal can be taken to be $\theta = \cos^{-1}[k_n/K(z)]$. For a simple isovelocity waveguide, the maximum sound speed is the bottom sound speed corresponding to min $[K(z)]$. At this value of $K(z)$, we have from Snell's law $\theta = \theta_c$, the bottom critical angle. In effect, if we look at a ray picture of the modes, the continuous portion of the mode spectrum corresponds to rays with grazing angles greater than the bottom critical angle of Fig. 2(b) and therefore outside the cone of Fig 3(a). This portion undergoes severe loss. Hence, we note that the continuous spectrum is the near (vertical) field and the discrete spectrum is the [more horizontal, profile-dependent) far field [falling within the cone in Fig. 3(a)].

The advantages of the NM procedure are that:

- the solution is available for all source and receiver configurations once the eigenvalue problem is solved;
- it is easily extended to moderately range-dependent conditions by using the adiabatic approximation; and
- it can be applied (with more effort) to extremely range-dependent environments using coupled mode theory.

However, it does not include a full representation of the near field.

Adiabatic and Coupled Mode Theory

All of the range-independent normal mode "machinery" developed for environmental ocean acoustic modeling applications can be adapted to mildly range-dependent conditions by using adiabatic mode theory. The underlying assumption is that individual propagating normal modes adapt (but do not scatter or "couple" into each other) to the local environment. The coefficients of the mode expansion, α in Eq. (35), now become mild functions of range, i.e., $a_n(\mathbf{k}) \rightarrow a_n(\mathbf{k}, \mathbf{r})$. This modifies Eq. (39) as follows:

$$G(\mathbf{r},z) = \frac{i\rho(z_s)}{(8\pi r)^{1/2}}\exp(-i\pi/4) \times \sum_n \frac{u_n(z_s)v_n(z)}{\overline{k_n}^{1/2}}\exp(i\overline{k_n} r - \overline{\alpha_n} r), \quad (41)$$

where the range-averaged eigenvalues and attenuation coefficients are

$$\overline{k_n} = \frac{1}{r}\int_0^r k_n(r')dr'; \quad \overline{\alpha_n} = \frac{1}{r}\int_0^r \alpha_n(r')dr', \quad (42)$$

and the $k_n(r')$, $\alpha_n(r')$ are obtained at each range segment from the eigenvalue problem [Eq. (36)] evaluated at the environment at that particular range along the path. The quantities u_n and v_n are the sets of modes at the source and the field positions, respectively.

UNCLASSIFIED

UNCLASSIFIED

UNCLASSIFIED

Simply stated, the adiabatic mode theory leads to a description of sound propagation such that the acoustic field is a function of the modal structure at both the source and the receiver and some average propagation between the two. Thus, for example, when sound emanates from a shallow region where only two discrete modes exist and propagates into a deeper region with the same bottom (same critical angle), the two modes from the shallow region adapt to the form of the first two modes in the deep region. However, the deep region can support many more modes. Intuitively, we therefore expect that the resulting two modes in the deep region will take up a smaller more horizontal part of the cone of Fig. 3(a) than they take up in the shallow region. This means that sound rays going from shallow to deep tend to become more horizontal, which is consistent with a ray picture of downslope propagation.

Finally, fully coupled mode theory[16] for range-dependent environments has been developed but requires additional intensive computation. The computational burden originates from having to include coupling in the backward as well as forward direction. Under certain conditions, restricting the computation to forward coupling results in a computationally tractable procedure. For example, forward coupled-mode theory has been applied to model pulse propagation for shallow-water tomography studies.[17]

PARABOLIC EQUATION MODEL (PE)

Standard PE-Split Step Algorithm

The PE method is a practical wave-theoretic range-dependent propagation model. In its simplest form, it is a farfield narrow-angle ($\sim \pm 15$ deg with respect to the horizontal—adequate for many underwater propagation problems) approximation to the wave equation. Assuming azimuthal symmetry about a source, we express the solution of Eq. (27) in cylindrical coordinates in a source-free region in the form

$$G(r,z) = \psi(r,z) \cdot J(r), \tag{43}$$

and we define $K^2(r,z) \equiv K_0^2 n^2$, n therefore being an "index of refraction" c_0/c, where c_0 is a reference sound speed. Substituting Eq. (43) into Eq. (27) in a source-free region and taking K_0^2 as the separation constant, J and ψ satisfy the following two equations:

$$\frac{d^2J}{dr^2} + \frac{1}{r}\frac{dJ}{dr} + K_0^2 J = 0; \tag{44}$$

$$\frac{\partial^2\psi}{\partial r^2} + \frac{\partial^2\psi}{\partial z^2} + \left[\frac{1}{r} + \frac{2}{J}\frac{\partial J}{\partial r}\right] + \frac{\partial\psi}{\partial r} + K_0^2 n^2 \psi - K_0^2\psi = 0. \tag{45}$$

Equation (44) is a Bessel equation, and we take the outgoing solution, a Hankel function $H_0^1(K_0 r)$, in its asymptotic form [given above Eq. (33)] and substitute it into Eq. (45), together with the "paraxial" (narrow angle) approximation

$$\frac{\partial^2\psi}{\partial r^2} \ll 2K_0 \frac{\partial\psi}{\partial r} \tag{46}$$

to obtain the parabolic equation (in r),

$$\frac{\partial^2\psi}{\partial z^2} + 2iK_0 \frac{\partial\psi}{\partial r} + K_0^2(n^2 - 1)\psi = 0, \tag{47}$$

where we note that n is a function of range and depth. Here, we use the "split-step" marching solution[18] to solve the parabolic equation. We take n to be a constant for each range step; the error this introduces can be made arbitrarily small by the appropriate numerical gridding. The Fourier transform of ψ can then be written as

$$\chi(r,s) = \frac{1}{2\pi}\int_{-\infty}^{\infty} \psi(r,z)\, \exp(-isz)dz \tag{48}$$

which together with Eq. (47) gives

$$-s^2\chi + 2iK_0 \frac{\partial\chi}{\partial r} + K_0^2(n^2 - 1)\chi = 0. \tag{49}$$

The solution of Eq. (49) is simply

$$\chi(r,s) = \chi(r_0,s) \times \exp\left[-\frac{K_0^2(n^2 - 1) - s^2}{2iK_0}(r - r_0)\right], \tag{50}$$

UNCLASSIFIED

UNCLASSIFIED

UNCLASSIFIED

with specified initial condition at r_0. The inverse transform gives the field as a function of depth,

$$\psi(r,z) = \int_{-\infty}^{\infty} \chi(r_0,s) \exp\left[\frac{iK_0}{2}(n^2 - 1)\Delta r\right] \times \exp\left[-\frac{i\Delta r}{2K_0}s^2\right] \exp(isz)ds, \quad (51)$$

where $\Delta r = r - r_0$. Introducing the symbol $\mathcal{F}$ for the Fourier transform operation from the z-domain [as performed in Eq. (48)] and $\mathcal{F}^{-1}$ as the inverse transform, Eq. (51) can be summarized by the range-stepping algorithm,

$$\psi(r + \Delta r,z) = \exp\left[\frac{iK_0}{2}(n^2 - 1)\Delta r\right] \times \mathcal{F}^{-1}\left[\left[\exp\left(-\frac{i\Delta r}{2K^0}s^2\right)\right] \cdot \mathcal{F}[\psi(r,z)]\right], \quad (52)$$

which is often referred to as the "split step" marching solution to the PE. The Fourier transforms are performed using FFTs. Equation (52) is the solution for n constant, but the error introduced when n (profile or bathymetry) varies with range and depth can be made arbitrarily small by increasing the transform size and decreasing the range-step size.

Finally, since the PE is an initial value problem, we must have a starting field. Typically we can approximate a point source as a Gaussian shape since we are only concerned with propagation angles confined to the narrow cone discussed in this paper:[3]

$$\psi(0,z) = \sqrt{K_0}\, e^{-\frac{K_0^2}{2}(z - z_s)^2}. \quad (53)$$

When the source is near the surface, it is helpful to use an antisymmetric combination of the source and its image so that the surface boundary condition is satisfied,

$$\psi(0,z) = \psi(0,z - z_s) - \psi(0,z + z_s), \quad (54)$$

where z_s is the source depth. Another common method is to initialize the field with a normal mode representation. There are also more accurate and elegant methods to initialize the PE (refer to Chapter 6 of Ref. 3 for an assortment of methods).

Generalized or Higher Order PE Methods

Methods of solving the parabolic equation, including extensions to higher angle propagation,[19-22] elastic media,[23] and direct time-domain solutions with nonlinear effects[24] have recently appeared.

Equation (47), with the second-order range derivative that was neglected because of Ineq. (46), can be written in operator notation as

$$[P^2 + 2iK_0P + K_0^2(Q^2 - 1)]\,\psi = 0, \quad (55)$$

where

$$P \equiv \frac{\partial}{\partial r},\ Q \equiv \sqrt{n^2 + \frac{1}{K_0^2}\frac{\partial^2}{\partial z^2}}. \quad (56)$$

Factoring Eq. (55) assuming weak range-dependence and retaining only the factor associated with outgoing propagation yields a one-way equation

$$P\psi = iK_0(Q - 1)\psi, \quad (57)$$

which is a generalization of the parabolic equation beyond the narrow angle approximation associated with Ineq. (46). If we define $Q = \sqrt{1 + q}$ and expand Q in a Taylor series as a function of q, the standard PE method is recovered with $Q \approx 1 + .5q$. The wide-angle PE to arbitrary accuracy in angle, phase, etc., can be obtained from a Padé series representation of the Q operator,[19]

$$Q \equiv \sqrt{1+q} = 1 + \sum_{j=1}^{m} \frac{\alpha_{j,m}q}{1 + \beta_{j,m}q} + O(q^{2m+1}), \quad (58)$$

where m is the number of terms in the Padé expansion and

$$\alpha_{j,m} = \frac{2}{2m+1}\sin^2\left[\frac{j\pi}{2m+1}\right],\ \beta_{j,m} = \cos^2\left[\frac{j\pi}{2m+1}\right]. \quad (59)$$

UNCLASSIFIED

UNCLASSIFIED

UNCLASSIFIED

The solution of Eq. (57) using Eqs. (58)-(59) has been implemented using finite-difference techniques for fluid and elastic media.[19,23]

A numerical method that allows one to solve the PE with large range steps (although the environmental range-dependence must still be adequately sampled) has been recently developed and is referred to as the split-step Padé.[20,21] In this technique, Eq. (57) is integrated analytically,

$$P(r+\Delta r) = \exp\left[iK_0(-1+\sqrt{1+q})\right]P(r), \qquad (60)$$

and the the Padé approximation is then applied,

$$\exp[iK_0(-1+\sqrt{1+q})] \simeq \sum_{j=1}^{m} \frac{a_{j,m}q}{1+b_{j,m}q}, \qquad (61)$$

where the coefficients in the Padé series are discussed in Ref. 21. The split-step Padé formula is obtained by substituting Eq. (61) into Eq. (60),

$$P(r+\Delta r) = P(r) + \sum_{j=1}^{m} (a_{j,m})(1+b_{j,m}q)^{-1} q\, P(r). \qquad (62)$$

Range steps of more than an order of magnitude greater than that used in the previous Padé implementation are now permissible. Furthermore, the structure of the solution permits the efficient use of parallel processors to speed up execution of the algorithm. As far as the starting fields are concerned, the same issues apply as discussed in the previous subsection. However, the "self-starter" algorithm[22] is particularly useful.

Transmission Loss (TL)

The models discussed in this section compute complex quantities such as pressure. However, in underwater acoustics it is convenient to express the field in terms of transmission loss, which is defined as

$$TL(\mathbf{r},\mathbf{r}_s) = -20 \log_{10} \left| \frac{\rho(\mathbf{r},\mathbf{r}_s)}{p_0(\mathbf{r}_s)} \right|, \qquad (63)$$

where $p(\mathbf{r}, \mathbf{r}_s)$ is the acoustic pressure at point $\mathbf{r}$ from a simple point source at point $\mathbf{r}_s$, and $p_0(\mathbf{r}_0)$ is the pressure produced at a distance of 1 m from the same source in an infinite homogeneous medium with density $\rho(\mathbf{r}_s)$. Thus, we have that $p_0(\mathbf{r}_0) = (4\pi r)^{-1}\exp(iKr)$ with $r = 1$. This formula is also referred to as the coherent TL when applying it to normal mode models in that TL contains the variations resulting from interfering modes. The incoherent TL is obtained from a normal mode model by taking for the numerator the square root of the sum of the magnitudes squared of the individual modal terms in Eqs. (39) or (41).

Propagation of Pulses

Presently, the most practical method to compute the shape of a pulse as it propagates in shallow water is by Fourier synthesis. That is, a transmitted pulse with a source spectrum $f(\omega)$ will have a pulse shape at (r,z,t) given by

$$P(r,z,t) = \int_{-\infty}^{\infty} f(\omega)p(r,z;\omega)\, e^{-i\omega t}\, d\omega, \qquad (64)$$

where $p(r,z;\omega)$ is the acoustic field that can be computed from any of the wave models discussed in this section. In particular, a normal mode over moderate bandwidths can be used very efficiently by interpolating modal wavenumbers across frequency but assuming that the mode shapes do not significantly change. This interpolation has even been applied to coupled-mode computations.[17] Time series can also be generated efficiently using ray theory.[25]

SOME RESULTS

Range-Independent TL

It is well established that all the models should be in agreement for range-independent environments. In overlapping regions of validity (far field), normal mode and spectral (FFP) solutions are identical. It is only more recently the PE results have converged to give the same solution as a benchmark FFP solution. Figure 5 shows some results[3] for a 100-m Pekeris waveguide with source and receiver at a depth of 99.5 m (for maximum interference structure). The water and bottom speeds are 1500 and 1590 m/s, respectively; the density ratio between water and bottom is 1.2; and the bottom attenuation is 0.5 dB/λ. The frequency is 250 Hz. The standard PE without high angle accuracy fails to match the benchmark FFP results whereas the higher angle PE does.

UNCLASSIFIED

UNCLASSIFIED

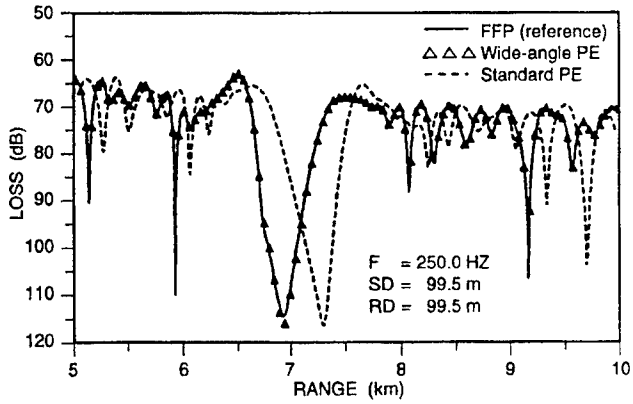

Fig. 5 — Comparison of transmission loss results for narrow and wide-angle PEs with FFP reference solution

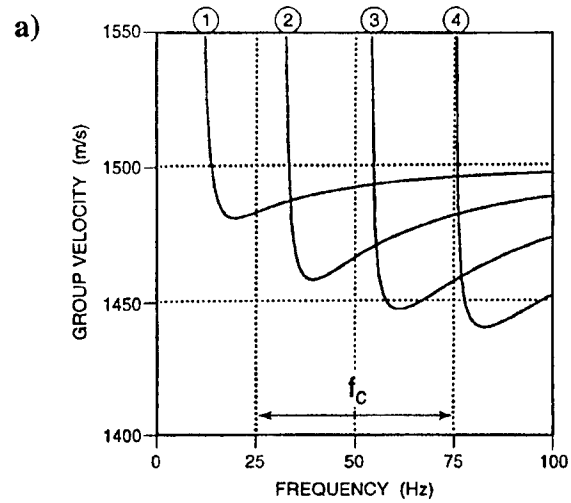

(a) Dispersion characteristics of the waveguide

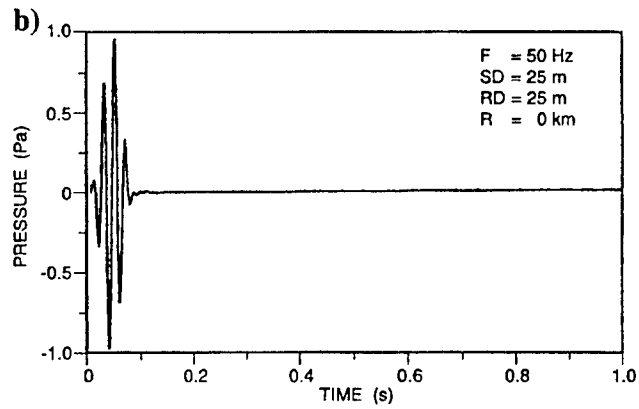

(b) Source pulse

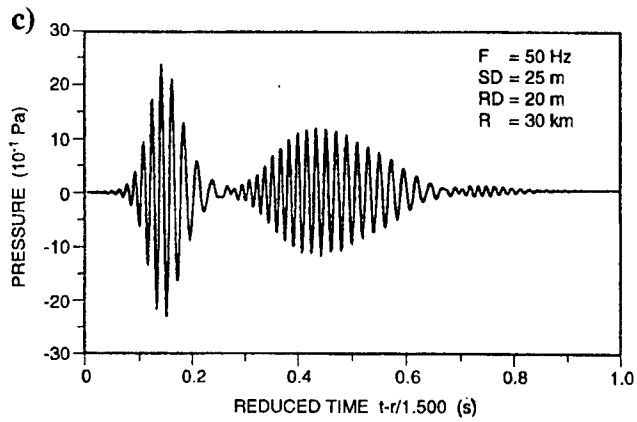

(c) Received signal at a distance of 30 km from the source.

Fig. 6 — 50 Hz bandwidth pulse propagation in a Pekeris waveguide.[3] The initial pulse length of 0.08 s becomes strongly dispersed, with a final length of around 0.7 s.

Bottom Shear Wave Effects

For ocean bottoms with at least some rigidity, the effect of the existence of shear provides the sound field with additional degrees of freedom to interact with the bottom. The mechanism is coupling into shear waves and/or interface waves (for a source acoustically close to the bottom interface). For bottoms with shear wave speeds less than the speed of sound in the water column, the shear waves carry energy away from the water column. The major effect is increased attenuation at low frequencies over nonshear-supporting ocean bottoms. For the case when the shear speed is higher than the water column sound speed, the ratio of water column sound speed to shear speed determines the critical angle. If a source is close (of the order of a wavelength) to the bottom, it will couple into an interface wave (Scholte wave at fluid-solid interface or Stoneley wave and solid-solid interface). These wave can be detected by hydrophones near or on the bottom or seismometers on the bottom. All these effects are computable using an FFP model.[12]

Broadband Modeling

Because modes travel at different phase and group speeds as a function of frequency, a pulse will disperse as it propagates. The phase speed is the horizontal propagation speed ($u_n = \omega/k_n$) of a wavefront [see, for example Fig. 3(b)] corresponding to a mode, whereas the group speed ($v_n = (dk_n/d\omega)^{-1}$) of a mode represents the speed at which an energy packet (which has a finite bandwidth) propagates down the waveguide. Figure 6 shows plots of modal group speeds and a dispersing pulse in a Pekeris waveguide.[3] The sound speeds in the water column and bottom are 1500 and

UNCLASSIFIED

1600 m/s, respectively. The density ratio is 1.5, and the bottom attenuation is 0.2 dB/λ. Here, we see that the initial pulse disperses into two distinct pulses (mode 1 and 2) as a result of the different modal group speeds. At the trailing tail is a weak third mode arrival.

We also should note that, in general, a good approximation to modeling TL over some bandwidth, say, a one-third octave band, is simply to compute the incoherent normal mode transmission loss at the center frequency.

Optimum Frequency

The tradeoff between high-frequency attenuation and scattering and low-frequency bottom loss leads to an optimum frequency of propagation in a waveguide. The optimum frequency in a shallow-water environment depends to a large extent on the width of the effective ducted propagation as well as the properties of the water column and bottom type. For a winter profile, the duct corresponds to the water depth. For a summer profile with source and receiver below the thermocline, the effective duct is the water column below the thermocline. Figure 7 is the results of an experimental and modeling study including a contour of third-octave TL vs frequency and range.[26] The optimum frequency is seen to be about in the region of 200-400 Hz from the contours. For example, at a range of about 60 km, the loss increases for frequencies above and below the optimum frequency of propagation. Agreement between experiment and theory was obtained by using the model/data comparison to fine-tune the bottom parameters. Of course, one set of bottom parameters must satisfy the data at all frequencies.

Range-Dependent TL

The PE is the most robust method for computing mid- to low-frequency TL in a range-dependent shallow-water environment. The April 1990 issue of the *Journal of the Acoustical Society of America* has a set of papers benchmarking various range-dependent models.[27] A range-dependent phenomenon of growing interest is the existence of internal wave solitons. These have been studied deterministically to demonstrate their acoustic influence. Using the parabolic equation and projecting the results into mode space, it has been shown that these solitons can explain measured data in such an environment.[28]

Three-Dimensional (3D) Propagation

All of the acoustic models we have discussed are two dimensional (2D), range and depth, which is often a good approximation. There are essentially two methods to treat a three-dimensionally varying environment. The most straightforward and still not very practical method is to formally solve the 3D wave equation for a 3D environment. This has been done to some extent using ray methods[29] but is still rather numerically intractable in the wave theoretic regime. An approximation is to compute 2D TL along radials and outward from a source.[30] Figure 8 shows an example of this for a bathymetrically variable shallow-water region.[31] TL loss computations along horizontal refracting paths have also been made using a new model referred to as the Adiabatic Mode PE.[32] This latter reference includes very-low-frequency deep-water computations that essentially scale to approximately the shallow-water acoustic regime.

SUMMARY

An assortment of models have been developed to compute the acoustic field in shallow-water environments in both the frequency and time domains. This paper has not considered fluctuations and other forms of statistical spatio-temporal variability of the environment/acoustics. The relationship between these models is well understood, and their accuracy as related to solving the wave equation is also understood. However, these models require environmental inputs—sound speeds and geophysical properties of the bottom as a function of position—which turn out to be the limiting factor in how well they model real-world scenarios.

REFERENCES

1. *Oceanographic and Atmospheric Master Library Summary*, OAML-SUM-21D, Naval Oceanographic Office, Systems Integration Department, Stennis Space Center, MS 39522-5001 (1995).

2. E. Chaika, Office of Naval Research, private communication (1996).

3. F.B. Jensen, W.A. Kuperman. M.B. Porter and H. Schmidt, *Computational Ocean Acoustics* (AIP Press, New York, 1994) [ISBN 1563962098].

4. "Overview of Selected Underwater Acoustic Propagation Models," Science Applications International Corporation (SAIC) McLean, VA 22101 (prepared for the Office of Naval Research, AEAS Program) (1993).

5. P.C. Etter, *Underwater Acoustic Modeling: Principles, Techniques and Applications*, second edition (Chapman and Hall, New York, NY, 1995) [ISBN:0419201904].

UNCLASSIFIED

UNCLASSIFIED

UNCLASSIFIED

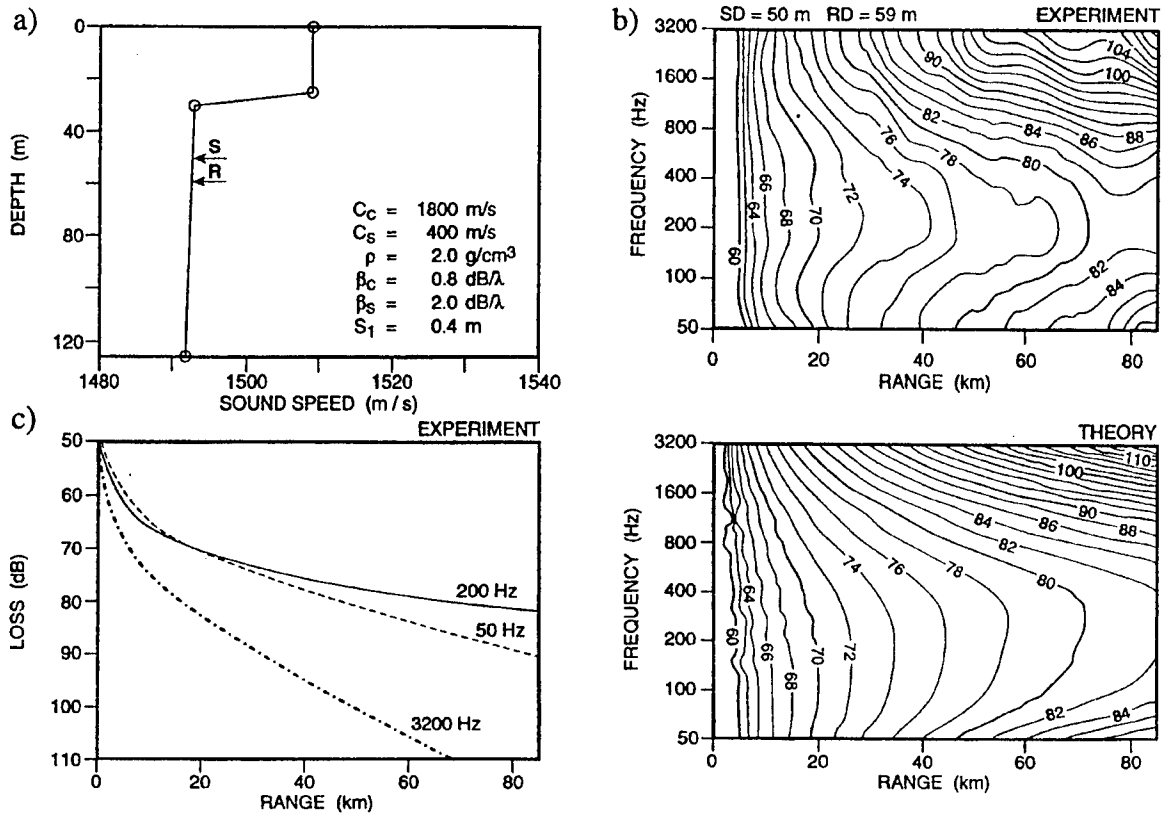

Fig. 7 — Optimum frequency. (a) Summer shallow-water environment; (b) Frequency vs depth propagation loss contours; experiment and model results; (c) Third octave propagation loss curves (which are horizontal cuts of contours

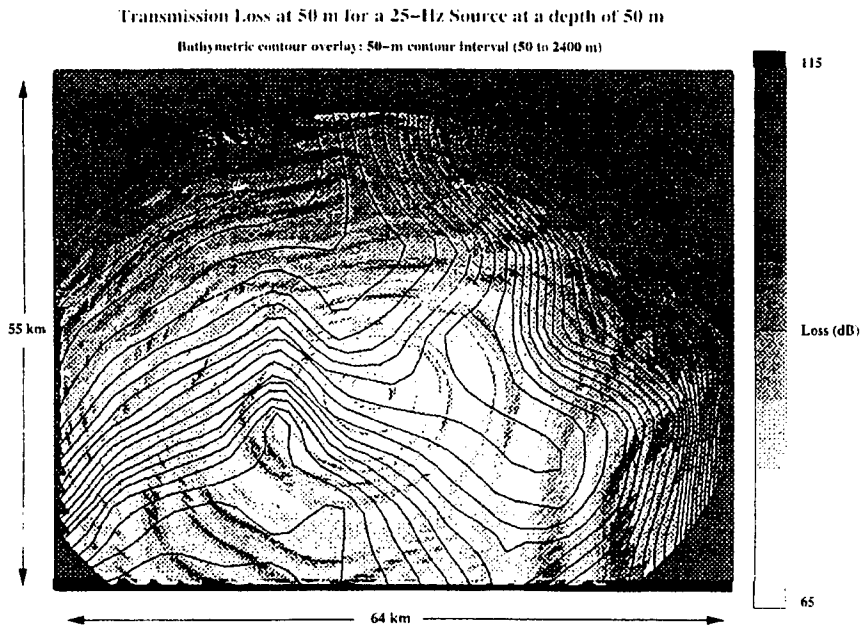

Fig. 8 — Transmission loss map constructed from adiabatic mode model

UNCLASSIFIED

UNCLASSIFIED

6. "APL-UW High-Frequency Ocean Environmental Acoustics Modules Handbook," APL-UW TR 9407/AEAS 9501, Applied Physics Laboratory, University of Washington, Seattle, Washington 98105-6698 (1994).

7. D.L. Bradley and R.J. Urick, "A Compilation of Acoustic Transmission Loss Measurements in Shallow Water," TR 68-180, Naval Ordnance Laboratory, White Oak, MD, 1968.

8. C.S. Clay and H. Medwin, *Acoustical Oceanography* (Wiley-Interscience, New York, NY, 1977).

9. L.M. Brekhovskikh and Yu. Lysanov, *Fundamentals of Ocean Acoustics*, second edition (Springer-Verlag, Berlin, Germany, 1991).

10. D.S. Ahluwalia and J.B. Keller, "Exact and Asymptotic Representations of the Sound Field in a Stratified Ocean," in *Wave Propagation in Underwater Acoustics*, edited by J.B. Keller and J.S. Papadakis (Springer-Verlag, New York, NY, 1977), pp. 14-85.

11. H. Schmidt and F.B. Jensen, "A Full Wave Solution for Propagation in Multilayered Viscoelastic Media with Application to Gaussian Beam Reflection at Fluid-Solid Interface," J. Acoust. Soc. Am. **77**, 813-825 (1985).

12. H. Schmidt, "OASES Version 1.7 Application and Upgrade Notes," technical report, Massachusetts Institute of Technology, Cambridge, MA (1995).

13. H. Schmidt, W. Seong, and J.T. Goh, "A Super-Element Approach to Range-Dependent Ocean Acoustic Modeling," J. Acoust. Soc. Am. **98**, 465-472 (1995).

14. H. Weinberg, "Effective Range Derivative for Acoustic Propagation Loss in a Horizontally Stratified Ocean," J. Acoust. Soc. Am. **70**, 1736-1742 (1981).

15. H. Weinberg, "Generic Sonar Model (GSM)," TD 5971D, Naval Underwater Systems Center, New London, CT (1985). See also "The CST Program Modeling Subsystem: Generic Sonar Model (GSM)," Science Applications International Corporation, Undersea Applications Modeling Division, McLean, VA (1991).

16. R.B. Evans, "A Coupled Mode Solution for Acoustic Propagation in a Waveguide with Stepwise Depth Variations of a Penetrable Bottom," J. Acoust. Soc. Am. **74**, 188-195 (1983).

17. C.S. Chiu, J.H. Miller, and J.F. Lynch, "Forward Coupled-Mode Propagation Modeling for Coastal Acoustic Tomography," J. Acoust. Soc. Am. **99**, 793-802 (1996).

18. F.D. Tappert "The Parabolic Equation Method," in *Wave Propagation in Underwater Acoustics*, edited by J.B. Keller and J.S. Papadakis (Springer-Verlag, New York, NY, 1977), pp. 224-287 (1977).

19. M.D. Collins, "Applications and Time-Domain Solution of Higher-Order Parabolic Equations in Underwater Acoustics," J. Acoust. Soc. Am. **86**, 1097-1102 (1989).

20. M.D. Collins, "A Split-Step Padé Solution for the Parabolic Equation Method," J. Acoust. Soc. Am. **93**, 1736-1742 (1993).

21. M.D. Collins, "Generalization of the Split-Step Padé Solution," J. Acoust. Soc. Am. **96**, 382-385 (1994).

22. M.D. Collins, "A Self Starter for the Parabolic Equation Method," J. Acoust. Soc. Am. **92**, 2069-2074 (1992).

23. M.D. Collins, "A Higher-Order Parabolic Equation for Wave Propagation in an Ocean Overlying an Elastic Bottom," J. Acoust. Soc. Am. **89**, 1050-1057 (1991).

24. B.E. McDonald and W.A. Kuperman, "Time Domain Formulation for Pulse Propagation Including Nonlinear Behavior at a Caustic," J. Acoust. Soc. Am. **81**, 1406-1417 (1987).

25. E.K. Westwood and C.T. Tindle, "Shallow Water Time-Series Simulation Using Ray Theory," J. Acoust. Soc. Am. **81**, 1752-1761 (1987).

26. F.B. Jensen and W.A. Kuperman, "Optimum Frequency of Propagation in Shallow Water Environments," J. Acoust. Soc. Am. **73**, 813-819 (1983).

27. F.B. Jensen and C.M. Ferla, "Numerical Solutions of Range-Dependent Benchmark Problems in Ocean Acoustics," J. Acoust. Soc. Am. **87**, 1499-1510 (1990) and the following six papers in this issue.

28. J. Zhou, X. Zhang, and P.H. Rogers, "Resonant Interaction of Sound Wave and Internal Solitons in the Coastal Zone," J. Acoust. Soc. Am. **90**, 2042-2054 (1991).

29. R.M. Jones, T.M. Georges, and J.P. Riley, "HARPO, a Versatile Three-Dimensional Hamiltonian Ray-Trace Program for Acoustic Waves in the Ocean with Arbitrary Bottom," NOAA Special Report, National Oceanographic and Atmospheric Administration (NOAA) Environmental Research Laboratory, Boulder, CO (1986), 455 pp.

30 W.A. Kuperman, M.B. Porter, J.S. Perkins, and R.B. Evans, "Rapid Computation of Acoustic Fields in Three-Dimensional Ocean Environments," J. Acoust. Soc. Am. **89**, 125-133 (1991).

31. J.S. Perkins, Naval Research Laboratory, unpublished communication (1996).

32. M.D. Collins, "The Adiabatic Mode Parabolic Equation," J. Acoust. Soc. Am. **94**, 2269-2278 (1993).

UNCLASSIFIED

Appendix

UNITS

The decibel (dB) is the dominant unit in underwater acoustics and denotes a ratio of intensities (not pressures) expressed in terms of a logarithmic (base 10) scale. Two intensities, I_1 and I_2, have a ratio, I_1/I_2, in decibels of 10 log I_1/I_2 dB. Absolute intensities can therefore be expressed by using a reference intensity. The presently accepted reference intensity is a micropascal (μPa): the intensity of a plane wave having an rms pressure equal to 10^{-5} dynes per square centimeter. Therefore, taking 1 μPa as I_2, a sound wave having an intensity, of, say, one million times that of a plane wave of rms pressure 1 μPa has a level of 10 log $(10^6/1) \equiv 60$ dB re 1 μPa. Pressure (p) ratios are expressed in dB re 1 μPa by taking 20 log p_1/p_2, where it is understood that the reference originates from the intensity of a plane wave of pressure equal to 1 μPa.

William A. Kuperman received B.S., M.S., and Ph.D. degrees in physics from the Polytechnic Institute of Brooklyn in 1965, the University of Chicago in 1966, and the University of Maryland in 1972, respectively. He joined the Acoustics Division of the Naval Research Laboratory (NRL) in 1967. In 1976 he went to the SACLANT Undersea Research Centre in La Spezia, Italy, for five years where he founded the Environmental Modeling Group. He returned to head the Numerical Modeling Division at what is now the NRL Detachment Stennis Space Center, MS. In 1985, he returned to NRL in Washington, DC. Since 1993, he has been a professor of oceanography and the director of the Marine Physical Laboratory of the University of California, San Diego. He has done theoretical and experimental ocean acoustic research on linear and nonlinear propagation, scattering, ambient noise, and signal processing.

UNCLASSIFIED

This Page Is

Intentionally

Left Blank